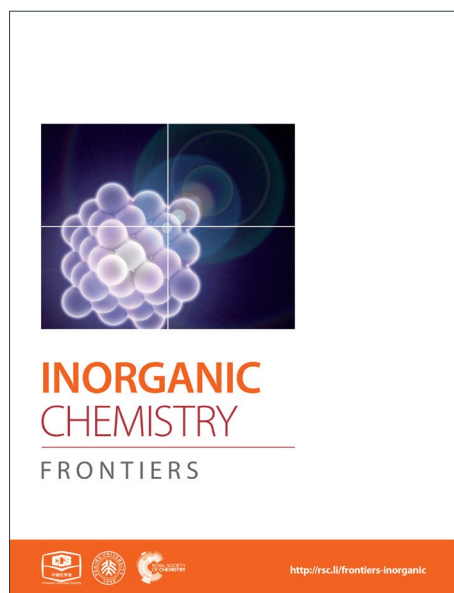
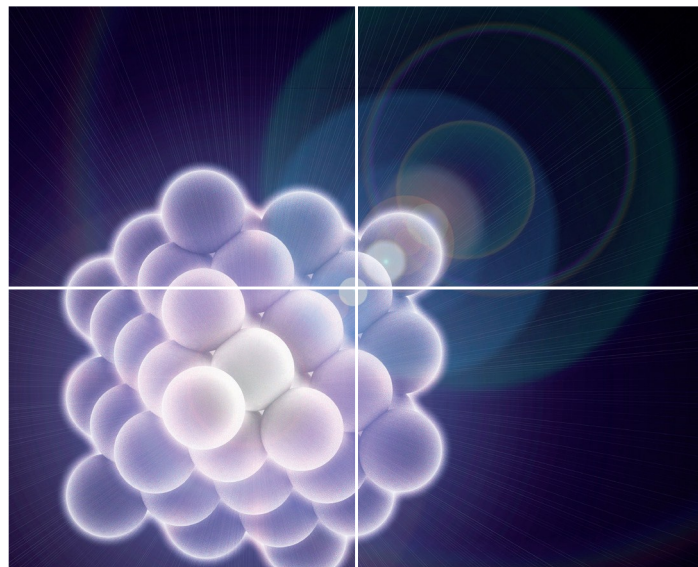


INORGANIC CHEMISTRY

FRONTIERS

Accepted Manuscript



This is an *Accepted Manuscript*, which has been through the Royal Society of Chemistry peer review process and has been accepted for publication.

Accepted Manuscripts are published online shortly after acceptance, before technical editing, formatting and proof reading. Using this free service, authors can make their results available to the community, in citable form, before we publish the edited article. We will replace this *Accepted Manuscript* with the edited and formatted *Advance Article* as soon as it is available.

You can find more information about *Accepted Manuscripts* in the [Information for Authors](#).

Please note that technical editing may introduce minor changes to the text and/or graphics, which may alter content. The journal's standard [Terms & Conditions](#) and the [Ethical guidelines](#) still apply. In no event shall the Royal Society of Chemistry be held responsible for any errors or omissions in this *Accepted Manuscript* or any consequences arising from the use of any information it contains.



Journal Name

COMMUNICATION

Water Adsorption Properties of a Sc(III) Porous Coordination Polymer for CO₂ Capture applications

Received 00th January 20xx,
Accepted 00th January 20xx

J. Raziel Álvarez,^a Ricardo A. Peralta,^a Jorge Balmaseda,^a Eduardo González-Zamora,^{*b} and Ilich A. Ibarra^{*a}

DOI: 10.1039/x0xx00000x

www.rsc.org/

Water adsorption at room temperature in NOTT-400 was investigated along with its ability to perform CO₂ capture in relative humidity (RH) conditions. Thus, the CO₂ capture was increased from 4.2 wt% (anhydrous conditions) to 10.2 wt% under 20 % RH at 30 °C.

Metal-organic frameworks (MOFs) or porous coordination polymers (PCPs) are very promising candidates for gas sequestration, since these materials show high sorption selectivity towards adsorbates. This selectivity can be adjusted as a function of the size, shape and chemical composition of the pores.¹ Although their potential as capture porous materials, many PCPs are unstable when exposed to moisture.^{2,3} Water could either shift the bound ligand, leading to the collapse of the PCP structure, or block the binding adsorption sites and therefore, avoid the adsorption of other desired molecules.³ Thus, water stability has limited the use of PCPs in industrial settings because moisture is ubiquitously in the environment and it must be accounted for adsorption, storage and separation systems. For example, natural gas streams are frequently saturated with water vapour that has to be removed (to ppm levels) before storage or use.⁴ Industrial flue gas, resulting from the combustions of fossil fuels, is saturated with water (5-7%).⁵

However, a significant number of PCPs have exhibited relatively good stability to water, for example: UiO-66,⁶ NOTT-401,⁷ MIL-100,⁸ MIL-101,⁹ MIL-53¹⁰ and InOF-1.¹¹ Thus, understanding and predicting the adsorption properties of water in hydrostable PCPs is fundamental for the development of industrial applications. Doonan and co-workers¹² showed a Cu(II) metal-organic framework (Cu(bcppm)H₂O, H₂bcppm = bis(4-(4-carboxyphenyl)-1H-pyrazolyl)methane) which is

hydrostable and also performed a remarkable selective separation of CO₂ from N₂. Walton and co-workers have shown water adsorption isotherms for a series of PCPs (Mg-MOF-174, DMOF-1, UiO-66 and UMCM-1) and compared them with reference micro-mesoporous materials.¹³ Farrusseng *et al.*¹⁴ reported structure property relationships of water adsorption in a comprehensive series of PCPs (MIL-53, MIL-68, MIL-101, MIL-125, etc.). Moreover, some of these water stable materials have been investigated for application in storage technologies for arid environments,¹⁵ heat-pumps and chillers,¹⁶ low-cost water capture¹⁵ and proton conductivity.¹⁷

The effect of water on the CO₂ capture has only recently been investigated on PCPs.¹⁸ Water adsorption is often unfavourable for CO₂ capture since water acts as a strong adsorptive competitor. However, LeVan,¹⁹ Matzger²⁰ and Walton²¹ demonstrated that controlled water adsorption can enhance CO₂ capture in PCPs. Llewellyn and co-workers²² investigated the CO₂ adsorption in some PCPs under different relative humidities of water vapour. Then, UiO-66 did not show any enhanced CO₂ uptake and for MIL-100(Fe), a remarkable 5-fold increase in CO₂ uptake was achieved. Interestingly, Walton and co-workers²³ showed hydroxyl functional groups act as a directing agent for water in the pores, which allows for more efficient packing. Furthermore, Yaghi *et al.*¹⁵ proposed that the presence of these functional groups, within the porous coordination polymer, enhance the affinity of the material for water. Thus, in the present work we have chosen a material entitled NOTT-400.^{24a} This material crystallises in the tetragonal tetragonal space group *I4*₁*22*, showing a binuclear [Sc₂(μ₂-OH)] building block (Figure S1, ESI[†]). The coordination around each Sc(III) centre is octahedral from six O-donors: 4 from different carboxylate groups and 2 from two μ₂-OH hydroxo groups which bridge two metal (Sc(III)) centres. NOTT-400 shows a three-dimensional framework structure with channel openings of approximately 8.1 Å (considering the van der Waals radii of the surface atoms).^{24a} We report herein the water adsorption properties and the CO₂ capture in the presence of water^{24b} in NOTT-400.

^a Instituto de Investigaciones en Materiales, Universidad Nacional Autónoma de México, Circuito Exterior s/n, CU, Del. Coyoacán, 04510, México D. F., Mexico
E-mail: argel@unam.mx

^b Departamento de Química, Universidad Autónoma Metropolitana-Iztapalapa, San Rafael Atlixco 186, Col. Vicentina, Iztapalapa, C. P. 09340, México D. F., Mexico.

[†] Footnotes relating to the title and/or authors should appear here.

Electronic Supplementary Information (ESI) available: TGA data, PXRD data and kinetic CO₂ experiments See DOI: 10.1039/x0xx00000x

First, the non-coordinated solvent molecules within the pores of the as-synthesised NOTT-400 were exchanged for acetone promoting accessibility to the desolvated framework after activation by heating. Thermogravimetric analysis (see Figure S2, ESI[†]) and bulk powder X-ray diffraction (PXRD) patterns (see Figure S3, ESI[†]) of as-synthesised and desolvated NOTT-400 confirmed that the material constantly maintains its structural integrity after desolvation. N₂ adsorption isotherms for activated NOTT-400 at 77 K were carried out in order to calculate the BET surface area ($0.01 < P/P_0 < 0.04$) of 1356 m² g⁻¹ (see Figure S8, ESI[†]) Water isotherms were performed on activated samples of NOTT-400 (see Experimental). Figure 1 shows the water adsorption isotherm of NOTT-400 at 30 °C. The adsorbed amount of water slowly increased with increasing pressure up to $\%P/P_0 = 20$. Thus, a rapid water uptake was observed in the pressure range from $\%P/P_0 = 20$ to 40. Finally, from $\%P/P_0 = 40$ to 90 there was a gradual weight increase, and the maximum water uptake was ~ 44.9 wt %. The overall water isotherm exhibited a sigmoidal shape and a relatively strong hysteresis loop (at $\%P/P_0 = 20-80$) was observed with marked stepped profiles in the desorption phase (Figure 1, open circles).

The pore openings in NOTT-400 (approximately 8.1 Å)^{24a} are considerably much larger than the kinetic diameter of water (~ 2.7 Å). Thus, in order to interpret this hysteresis loop, the arguments of 'kinetic trap', suggested by other research groups,²⁵ seem not to be suitable. Instead, the observed hysteresis is most likely due to moderately strong host-guest interactions, which result in an enhanced affinity of NOTT-400 for water. We believe that such interactions arise from the fact that water molecules can form hydrogen bonds with the bridging hydroxo functional groups (μ_2 -OH), within the pores, as previously described.²⁶

In addition, according to the crystal structure of NOTT-400^{24a} there are 8 hydroxo groups (μ_2 -OH) per unit cell. Thus, at low water loadings these groups can interact with water molecules representing the first domain (from 0 to approximately 32 $\%P/P_0$) of the water adsorption isotherm. The second domain, after the full coverage of the hydroxo functional groups with H₂O molecules, occurs at higher loadings. Thus, the slope of the isotherm grew abruptly due to stronger intermolecular interactions between water molecules affording condensation of water into the pores (Figure S5, see ESI[†]).

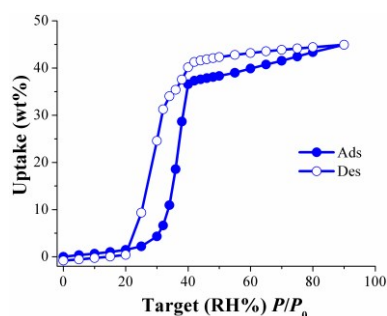


Figure 1. Water adsorption isotherm at 30 °C of NOTT-400. Solid circles represent adsorption, and open circles show desorption.

In order to measure the isosteric heat of adsorption for H₂O, we recorded a water adsorption isotherm at 20 °C (see Figure S9, ESI[†]) and the enthalpy for H₂O adsorption was calculated by fitting both isotherms (30 and 20 °C) to a Clausius-Clapeyron equation (see ESI[†]). The estimated enthalpy value was 46.8 kJ mol⁻¹ which is a typical value for PCPs.^{21d}

To test the water adsorption-desorption recyclability of NOTT-400 water sorption isotherms were measured, on the same sample, for 5 cycles at 30 °C (Figure 2). These results showed no apparent decrease in capacity over five cycles and revealed the complete regeneration of the material solely by evacuating for only 30 min without any thermal activation. In order to investigate any sample degradation, we have carried out PXRD experiments on the NOTT-400 sample after these cycling experiments. Figure S4 (see ESI[†]) confirms that the crystallinity of the sample after each water adsorption-desorption experiment (5 cycles) was retained.

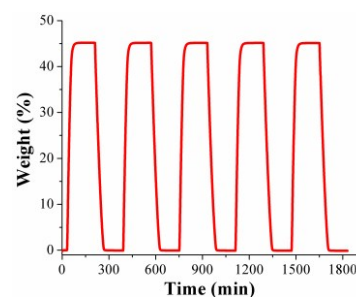


Figure 2. Water re-adsorption-desorption uptake on NOTT-400 at 30 °C.

Dynamic and isothermal CO₂ experiments were performed on NOTT-400 (see Experimental). In figure 3, a kinetic uptake experiment at 30 °C is shown. At this ambient temperature, the maximum amount of CO₂ captured under anhydrous conditions is 4.4 wt%, rapidly reached after only 7 min and it was constant until the end of the experiment at 60 min. In addition, we run CO₂ sorption experiments (adsorption/desorption) under static and isothermal conditions on NOTT-400 (see Fig. S10, ESI[†]). The CO₂ capture was 18.2 wt% which is significantly higher than under dynamic conditions (4.4 wt%). However, the central target of this paper is to exhibit, in a more realistic scenario, how NOTT-400 performs when it is exposed to a constant CO₂ flow gas (60 mL/min) and under water conditions.

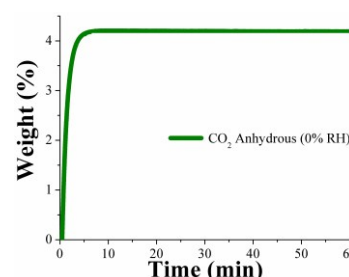


Figure 3. Kinetic uptake experiment performed at 30 °C with a CO₂ flow of 60 mL min⁻¹.

Kinetic isotherm experiments at 30 °C and different relative humidities (10, 20, 35 and 60 %RH) were carried out. We decided these RH values based on the water adsorption isotherm (see Figure 1): two values in the low loading region (10 and 20 %RH); one value in the middle of the sigmoidal-shaped isotherm (35 %RH) and finally one value in the high loading region (60 %RH). First, an activated NOTT-400 sample (180 °C for 1h and under a flow of N₂ gas) was stabilised at 30 °C and 10% RH. After the equilibrium was reached a constant CO₂ flow (60 mL min⁻¹) was carried out (see Figure 4, left).

In Figure 4 (left) the gradual weight increase (only H₂O) starts at 0 min and stabilised at around 15 min. In contrast, under anhydrous conditions the CO₂ uptake quickly reached stability (7 min, see Figure 3). Since the diffusion coefficient of water is smaller than CO₂, the vapour adsorption (water) process takes considerably more time to stabilise than the gas adsorption process in microporous materials.²⁷ Then, from 15 min to 50 min the H₂O uptake (0.7 wt%, which is in good agreement with the water adsorption isotherm; 0.67 wt%) was constant (plateau) and next, at 50 min the CO₂ flow (60 mL min⁻¹) was opened and a sharp weight gain, which reached stability at approximately 70 min, was observed (see Figure 4, left). We hypothesise that the adsorbed amount of H₂O is unchanged after the dosing of H₂O/CO₂ mixed gas as we observed earlier.²⁹ Then, from 70 min to 120 min (end of the experiment), the maximum amount of CO₂ captured (considering the water uptake of 0.7 wt%) corresponded to 7.8 wt%. Therefore, the CO₂ capture was approximately 2-fold increased with a 10 %RH (from 4.2 wt% to 7.8 wt%) in comparison to anhydrous conditions.

Later, kinetic CO₂ uptake experiments were performed on an activated sample of NOTT-400 at 30 °C and 20 %RH. Figure 4 (right) shows the gradual weight increase (H₂O) starting at 0 min and stabilised at around 15 min. From 15 to 50 min the water uptake was constant and equal to 1.5 wt% (in good agreement with the water adsorption isotherm value of 1.47 wt%). Then, the CO₂ flow was opened and abrupt uptake was observed (Figure 4 right). After stabilisation (after 70 min) the total CO₂ uptake was equal to 10.2 wt%. Thus, the CO₂ capture was approximately 2.5-fold increased (from anhydrous conditions to 20 %RH). This enhance in the CO₂ uptake in the presence of water can be explained by CO₂ confinements effects induced by water molecules.²⁸

Similarly, more kinetic CO₂ uptake isotherm experiments were carried out on activated samples of NOTT-400 at 30 °C and 35% RH (see Figure S6, ESI †) and 30 °C and 60% RH (see Figure S7, ESI †). The stabilisation times were 40 and 55 min (see Figure. S6 and S7, ESI †), respectively and in both cases after the CO₂ flow was started there was not a weight increase, meaning that CO₂ capture was not achieved at those relative humidities. At 35 and 60% RH, the water uptakes were 18.6 and 39.9 wt%, respectively. These values were in good agreement with the water adsorption isotherm, (see Figure 1) 18.72 and 39.88 wt%, respectively.

The porosity of NOTT-400 corresponds to the microporosity regime with a pore diameter of 8.1 Å.^{24a} The remarkable result

shown by Llewellyn and co-workers,²² increase in the CO₂ uptake, was reported in a mesoporous material at 40% RH and 30 °C (MIL-100(Fe)).²² This mesoporous material includes two types of cages of free openings of ~ 25 and 29 Å.²² We elucidated that at 35 and 60% RH the saturation of the micropores in NOTT-400, with H₂O molecules, was completed and thus, the inclusion of CO₂ molecules, into the micropores, was not possible. This explanation is supported by the experimental evidence that we previously reported²⁹ in another microporous material.

Additionally, Paesani *et al.*³⁰ investigated by computational infrared spectroscopy the behavior of water confined in a porous coordination polymer entitled MIL-53(Cr).³¹ Interestingly, MIL-53(Cr) is constructed with one-dimensional chains of corner-sharing CrO₄(μ₂-OH) octahedra, linked by 1,4-benzenedicarboxylate (BDC) ligands.³¹ Thus, they demonstrated³⁰ that water molecules (at low water loadings) interact strongly with the framework, *via* hydrogen bonding between the μ₂-OH functional group and H₂O, whereas intermolecular interactions between H₂O molecules become considerably stronger at higher loading. In other words, at low water loadings the MIL-53(Cr) channels provide a template for packing more efficiently water molecules and therefore, these H₂O molecules can then donate a hydrogen bond to the CO₂ molecules enhancing the total CO₂ uptake. These results correlate and support our experimental evidence.

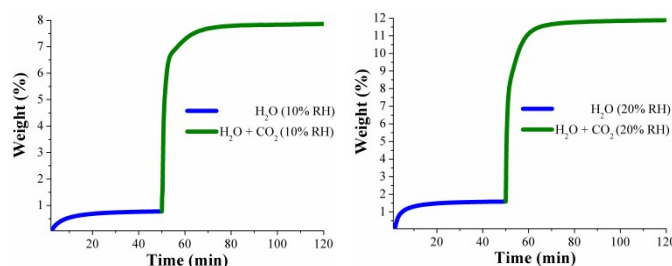


Figure 4. Kinetic uptake experiments carried out at 10 and 20% RH (both experiments at 30 °C); H₂O (blue line) and H₂O+CO₂ (green line).

Conclusions

In summary, the hydrostable the Sc(III) coordination polymer, NOTT-400, has permitted an evaluation of how porous coordination polymers can be used in the sorption of water at ambient temperature. NOTT-400 carries out CO₂ sequestration under relative humidity conditions. Finding the best partial saturation of H₂O molecules (percentage of relative humidity) into the micropores of NOTT-400 is crucial to increase the CO₂ uptake. Thus, after testing different relative humidity conditions (60, 35, 20 and 10% RH), we found that the maximum CO₂ capture was obtained at 20% RH and 30 °C with a total amount of ~10.2 wt %. Considerably, this CO₂ capture, under humid conditions, represents a 2.5-fold increase in comparison to anhydrous conditions. The CO₂ confinement effects induced by H₂O²⁸ can occur within the micropores of NOTT-400 enhancing the total CO₂ uptake.

Experimental Section

Water Adsorption Experiments.

Water vapour isotherms were recorded by a dynamic method, using air gas as carrier gas, in a DVS Advantage 1 instrument from Surface Measurement System (mass sensitivity: 0.1 μg , Relative Humidity (RH), accuracy: 0.5 %RH, vapour pressure accuracy: 0.7 % P/P_0). The hydration-dehydration cycles were measured in the same instrument. The water uptake in weight percent (wt%) units was calculated as [(adsorbed amount of water) / (amount of adsorbent) X 100], consistent with established procedures.

CO₂ Capture Experiments

Kinetic uptake experiments were performed by using a thermobalance (Q500 HR, from TA) at room temperature (30 °C) with a constant CO₂ flow (60 mL min⁻¹). Then, samples of NOTT-400 and were placed inside the thermobalance and activated by heating from room temperature to 180 °C for 1h and under a flow of N₂ gas. After the activated sample was cooled down, the desired temperature was set (30 °C) and a constant CO₂ flow (60 mL min⁻¹) was carried out. With a humidity-controlled thermobalance (Q5000 SA, from TA) kinetic uptake experiment at 30 °C with a constant CO₂ flow (60 mL min⁻¹) were performed on activated samples (180 °C for 1h and under a flow of N₂ gas) of NOTT-400.

Acknowledgements

The authors thank Dr. A. Tejeda-Cruz (X-ray; IIM-UNAM), CONACyT Mexico (212318), PAPIIT UNAM Mexico (IN100415) for financial support. J. B. thanks SEP-CONACyT (154626) and UNAM-DGAPA-PAPIIT (IG-100315). E.G-Z. thanks CONACyT (156801 and 236879), Mexico for financial support. Thanks to U. Winnberg (ITAM and ITESM) for scientific discussions.

Notes and references

- a) S. Yang, G. S. B. Martin, G. J. J. Titman, A. J. Blake, D. R. Allan, N. R. Champness and M. Schröder, *Inorg. Chem.*, 2011, **50**, 9374-9384; b) A. J. Nuñez, L. N. Shear, N. Dahal, I. A. Ibarra, J. W. Yoon, Y. K. Hwang, J.-S. Chang and S. M. Humphrey, *Chem. Commun.*, 2011, **47**, 11855-11857 (c) I. A. Ibarra, K. E. Tan, K. V. M. Lynch and S. M. Humphrey, *Dalton Trans.*, 2012, **41**, 3920-3923.
- J. J. Low, A. I. Benin, P. Jakubczak, J. F. Abrahamian, S. A. Faheem and R. R. Willis, *J. Am. Chem. Soc.*, 2009, **131**, 15834-15842.
- J. Cavinet, A. Feteeva, Y. Guo, B. Coasne and D. Farrusseng, *Chem. Soc. Rev.*, 2014, **43**, 5594-5617.
- A. M. Ribeiro, T. P. Sauer, C. A. Grande, R. F. P. M. Moreira, J. M. Loureiro and A. E. Rodriguez, *Ind. Eng. Chem.*, 2008, **47**, 7019-7026.
- a) K. Sumida, D. L. Rogow, J. A. Mason, T. M. McDonald, E. D. Bloch, Z. R. Herm, T.-H. Bae and J. R. Long *Chem. Rev.*, 2011, **112**, 724-781; b) R. S. Haszeldine, *Science*, 2009, **325**, 1647-1652.
- J. H. Cavka, S. Jakobsen, U. Olsbye, N. Guillou, C. Lamberti, S. Bordiga and K. P. Lillerud, *J. Am. Chem. Soc.* 2008, **130**, 13850-13851.
- H. A. Lara-García, M. R. Gonzalez, J. H. González-Estefan, P. Sánchez-Camacho, E. Lima and I. A. Ibarra, *Inorg. Chem. Front.*, 2015, **2**, 442-447.
- K. A. Cychosz and A. J. Matzger, *Langmuir*, 2010, **26**, 17198-17202.
- D.-Y. Hong, Y. K. Hwang, C. Serre, G. Férey and J.-S. Chang, *Adv. Funct. Mater.*, 2009, **19**, 1537-1552.
- J. Liu, F. Zhang, X. Zou, G. Yu, N. Zhao, S. Fan and G. Zhu, *Chem. Commun.*, 2013, **49**, 7430-7432.
- J. Qian, F. Jiang, D. Yuan, M. Wu, S. Zhang, L. Zhang and M. Hong, *Chem. Commun.*, 2012, **48**, 9696-9698.
- W. M. Bloch, R. Babaro, M. R. Hill, C. J. Doonan and C. J. Sumbly, *J. Am. Chem. Soc.*, 2013, **135**, 10441-10448.
- P. M. Schoenecker, C. G. Carson, H. Jasuja, C. J. J. Flemming and K. S. Walton, *Ind. Energ. Chem. Res.*, 2012, **51**, 6513-6519.
- J. Cavinet, J. Bonnefoy, C. Daniel, A. Legrand, B. Coasne and D. Farrusseng, *New J. Chem.*, 2014, **38**, 31012-3111.
- H. Furukawa, F. Gándara, Y.-B. Zhang, J. Jiang, W. L. Queen, M. R. Hudson and O. M. Yaghi, *J. Am. Chem. Soc.*, 2014, **136**, 4369-4381.
- a) F. Meunier, *Appl. Therm. Eng.*, 2013, **61**, 830-836; b) C. Janiak, and S. K. Henninger, *Chimia*, 2013, **67**, 419-424.
- M. Sadakiyo, H. Ōkawa, A. Shigematsu, M. Ohba, T. Yamada and H. Kitagawa, *J. Am. Chem. Soc.*, 2012, **134**, 5472-5475.
- a) S.-i. Noro, R. Matsuda, Y. Hijikata, Y. Inubushi, S. Takeda, S. Kitagawa, Y. Takahashi, M. Yoshitake, K. Kubo and T. Nakamura, *ChemPlusChem*, 2015, **80**, 1517; b) D. Kim, Y.-H. Ahn and H. Lee, *J. Chem. Eng. Data*, 2015, **60**, 2178; c) J. A. Mason, T. M. McDonald, T.-H. Bae, J. E. Bachman, K. Sumida, J. J. Dutton, S. S. Kaye and J. R. Long, *J. Am. Chem. Soc.*, 2015, **137**, 4787.
- a) J. Liu, A. I. Benin, A. M. B. Furtado, P. Jakubczak, R. R. Willis and M. D. LeVan, *Langmuir*, 2011, **27**, 11451-11456; b) J. Liu, Y. Wang, A. I. Benin, P. Jakubczak, R. R. Willis and M. D. LeVan, *Langmuir*, 2010, **26**, 14301-14307.
- A. C. Kizzie, A. G. Wong-Foy and A. J. Matzger, *Langmuir*, 2011, **27**, 6368-6373.
- a) H. Jasuja, Y.-G. Huang and K. S. Walton, *Langmuir*, 2012, **28**, 16874-16880; b) H. Jasuja, J. Zang, D. S. Sholl and K. S. Walton, *J. Phys. Chem. C*, 2012, **116**, 23526-23532; c) J. B. DeCoste, G. W. Peterson, H. Jasuja, T. G. Glover, Y.-G. Huang and K. S. Walton, *J. Mater. Chem. A*, 2013, **1**, 5642-5650; d) N. C. Burtch, H. Jasuja and K. S. Walton, *Chem. Rev.*, 2014, **114**, 10575-10612.
- E. Soubeyrand-Lenoir, C. Vagner, J. W. Yoon, P. Bazin, F. Ragon, Y. K. Hwang, C. Serre, J.-S. Chang and P. L. Llewellyn, *J. Am. Chem. Soc.* 2012, **134**, 10174-10181.
- G. E. Cmarik, M. Kim, S. M. Cohen and K. S. Walton, *Langmuir*, 2012, **28**, 15606-15613.
- a) I. A. Ibarra, S. Yang, X. Lin, A. J. Blake, P. J. Rizkallan, H. Nowell, D. R. Allan, N. R. Champness, P. Hubberstey and M. Schröder, *Chem. Commun.*, 2011, **47**, 8304-8306; b) M. R. Gonzalez, J. H. González-Estefan, H. A. Lara-García, P. Sánchez-Camacho, E. I. Basaldella, H. Pfeiffer and I. A. Ibarra, *New. J. Chem.*, 2015, **39**, 2400.
- a) X. B. Zhao, B. Xiao, A. J. Fletcher, K. M. Thomas, D. Bradshaw and M. J. Rosseinsky, *Science*, 2004, **306**, 1012-1015; b) H. J. Choi, M. Dincă and J. R. Long, *J. Am. Chem. Soc.*, 2008, **130**, 7848-7850.
- V. Haigis, F.-X. Coudert, R. Vuilleumier and A. Boutin, *Phys. Chem. Chem. Phys.*, 2013, **15**, 19049-19056.
- I. P. O'koye, M. Benham and K. M. Thomas, *Langmuir*, 1997, **13**, 4054-4059.
- a) N. L. Ho, F. Porcheron and R. J.-M. Pellenq, *Langmuir*, 2010, **26**, 13287-13296; b) L. N. Ho, J. Perez-Pellitero, F. Porcheron and R. J.-M. Pellenq, *Langmuir*, 2011, **27**, 8187-8197; c) L. N. Ho, S. Clauzier, Y. Schuurman, D. Farrusseng and B. Coasne, *J. Phys. Chem. Lett.*, 2013, **4**, 2274-2278.
- R. A. Peralta, B. Alcántar-Vázquez, M. Sánchez-Serratos, E. González-Zamora and I. A. Ibarra, *Inorg. Chem. Front.*, 2015, **2**, 898.
- G. R. Medders and F. Paesani, *J. Phys. Chem. Lett.*, 2014, **5**, 2897-2902.
- C. Serre, F. Millange, C. Thouvenot, M. Noguès, G. Marsolier, D. Louer and G. Férey, *J. Am. Chem. Soc.*, 2002, **124**, 13519-13526.